dairy

IMPACT FACTOR 3.1

CITESCORE 4.9

Article

Development of a Hybrid System Based on the CIELAB Colour Space and Artificial Neural Networks for Monitoring pH and Acidity During Yogurt Fermentation

Ulises Alvarado, Jhon Tacuri, Alejandro Coloma, Edgar Gallegos Rojas, Herbert Callo, Cristina Valencia-Sullca, Nancy Curasi Rafael and Manuel Castillo

MDPI

https://doi.org/10.3390/dairy6040041

dairy

MDPI

Article

Development of a Hybrid System Based on the CIELAB Colour Space and Artificial Neural Networks for Monitoring pH and Acidity During Yogurt Fermentation

Ulises Alvarado [1,2,*], Jhon Tacuri [1], Alejandro Coloma [1,2], Edgar Gallegos Rojas [1,2], Herbert Callo [1,2], Cristina Valencia-Sullca [3], Nancy Curasi Rafael [4] and Manuel Castillo [5]

1 Escuela Profesional de Ingeniería Agroindustrial, Facultad de Ciencias Agrarias, Universidad Nacional del Altiplano, Av. Floral 1153, Puno 21001, Peru; jtacurim@est.unap.edu.pe (J.T.); acoloma@unap.edu.pe (A.C.); edgallegosr@unap.edu.pe (E.G.R.); herbert.callo@unap.edu.pe (H.C.)
2 Instituto de Investigacion e Innovación en Producción, Seguridad Alimentaria y Agroindustria—IPSAA, Universidad Nacional del Altiplano, Av. Floral 1153, Puno 21001, Peru
3 Institut de Chimie & Biologie des Membranes et des Nano-objets (CBMN), UMR 5248, CNRS, Université de Bordeaux, Bordeaux INP, IECB, Allée Geoffroy Saint-Hilaire, F-33600 Pessac, France; cristina.valencia-sullca@u-bordeaux.fr
4 Escuela de Ingeniería Ambiental, Universidad Peruana Unión, Av. Héroes de la Guerra del pacifico, Juliaca 21100, Peru; ncurasi@upeu.edu.pe
5 Centre d'Innovació, Recerca i Transferència en Tecnologia dels Aliments (CIRTTA), Department of Animal and Food Sciences, Universitat Autònoma de Barcelona, Bellaterra, (Cerdanyola del Vallès), 08193 Barcelona, Spain; manuel.castillo@uab.es
* Correspondence: ualvarado@unap.edu.pe; Tel.: +51-99-3370-388

Abstract

Monitoring pH and acidity during yoghurt fermentation is essential for product quality and process efficiency. Conventional measurement methods, however, are invasive and labour-intensive. This study developed artificial neural network (ANN) models to predict pH and titratable acidity during yoghurt fermentation using CIELAB colour parameters (L, a*, b*). Reconstituted milk powder with 12% total solids was prepared with varying protein levels (4.2–4.8%), inoculum concentrations (1–3%), and fermentation temperatures (36–44 °C). Data were collected every 10 min until pH 4.6 was reached. Forty models were trained for each output variable, using 90% of the data for training and 10% for validation. The first two phases of the fermentation process were clearly distinguishable, lasting between 4.5 and 7 h and exceeding 0.6% lactic acid in all treatments evaluated. The best pH model used two hidden layers with 28 neurons (R^2 = 0.969; RMSE = 0.007), while the optimal acidity model had four hidden layers with 32 neurons (R^2 = 0.868; RMSE = 0.002). The strong correlation between colour and physicochemical changes confirms the feasibility of this non-destructive approach. Integrating ANN models and colourimetry offers a practical solution for real-time monitoring, helping improve process control in industrial yoghurt production.

Keywords: fermentation; pH; acidity; CIELAB colour space; artificial neural networks

Academic Editor: Adriano Gomes da Cruz

Received: 8 June 2025
Revised: 13 July 2025
Accepted: 24 July 2025
Published: 1 August 2025

Citation: Alvarado, U.; Tacuri, J.; Coloma, A.; Gallegos Rojas, E.; Callo, H.; Valencia-Sullca, C.; Rafael, N.C.; Castillo, M. Development of a Hybrid System Based on the CIELAB Colour Space and Artificial Neural Networks for Monitoring pH and Acidity During Yogurt Fermentation. *Dairy* **2025**, *6*, 41. https://doi.org/10.3390/dairy6040041

1. Introduction

Yogurt originated as an ancient method for preserving milk, dating back to around 6000 years B.C. in the Middle East [1,2]. Today, it ranks among the most widely consumed dairy products globally, owing to its nutritional, functional [3,4], and sensory qualities that

are highly valued by consumers [5–8]. Reflecting this growing demand, global yogurt sales are projected to exceed USD 237 billion by 2028 [9].

Fermentation constitutes the most critical phase in yogurt production, during which a viscous gel with distinctive flavour and high nutritional value is formed [10]. This process begins with the inoculation of symbiotic lactic acid bacteria, primarily from the *Lactobacillus* and *Streptococcus* genera [11], under controlled conditions typically ranging from 35 to 45 °C [12]. These parameters directly influence microbial growth, metabolic activity [13], and the bioconversion of lactose into lactic acid. As fermentation progresses, the pH gradually declines until the isoelectric point of casein is reached (pH 4.6) [4], thereby intensifying protein precipitation and triggering gelation through the formation of three-dimensional networks, a phenomenon that signifies the conclusion of fermentation [5,7,14]. Accordingly, both pH and titratable acidity are essential parameters for process monitoring and ensuring product safety.

In industrial settings, pH and acidity are traditionally measured discontinuously using electrochemical probes and titration techniques. Although these methods are reliable and accurate, they require frequent sampling, trained personnel, and laboratory analysis, making them time-consuming, labour-intensive, and inherently destructive [15]. In response, the industry has introduced in-line sensors that enable real-time pH monitoring when installed at critical control points within fermentation tanks. However, these systems present notable limitations, such as protein accumulation on the sensor surface, necessitating regular cleaning and recalibration [16], and the fragility of glass probes, which poses a risk of physical contamination.

To address these challenges, effective process control during fermentation necessitates tools that are capable of real-time, continuous, and accurate monitoring, while minimizing sample preparation and product waste. A promising and innovative approach would involve integrating an established technique such as colourimetry with an emerging technology such as artificial neural networks (ANNs). First, CIELAB-based colourimetry is a three-dimensional colour space with orthogonal coordinates: L* (lightness, from 0 for black to 100 for white), a* (green–red; negative for green, positive for red), and b* (blue–yellow; negative for blue, positive for yellow). Previous studies have demonstrated that these colour values change significantly during yogurt fermentation [17]. These variations can be used as indirect indicators of the fermentation progress, especially when combined with acidity and pH analyses. Secondly, artificial neural networks (ANNs) have gained increasing interest in the food industry due to their ability to detect nonlinear patterns, process large datasets, and emulate human-like decision-making, supporting continuous improvement processes [18]. This technology has been applied at various stages of dairy production. Notable applications include the prediction of disease (bovine tuberculosis) in dairy cows [19], as well as the prediction of milk production in Holstein cows [20]. It has also been used to determine the mineral profile of milk [21], predict optimal ripening time in cheese [22], estimate sensory attributes of yogurt [23], its textural properties [24], and storage time [25]. Furthermore, it has been applied to classify heat-treated milk [26], estimate casein content in milk [27], among other uses. These studies clearly demonstrate the relevance and effectiveness of ANNs.

However, to date, no study has explored the integration of ANNs with colourimetry based on the CIELAB system to monitor the yogurt fermentation process, representing an innovative opportunity for the development of non-destructive tools to predict pH and titratable acidity during yogurt fermentation.

In this context, the aim of the present study was to develop a predictive system that combines both technologies as a simple, rapid, cost-effective, and non-destructive

methodology, with potential for integration into automated real-time monitoring systems in industrial yogurt production.

2. Materials and Methods

2.1. Experimental Design

A completely randomized factorial design was employed, with all treatments conducted in triplicate, to assess the feasibility of the CIELAB colour system for monitoring pH and titratable acidity during low-fat yogurt fermentation. Fermentations were performed by combining three temperature levels (36, 40, and 44 °C), three protein concentrations (4.2%, 4.5%, and 4.8%), and three inoculum levels (1%, 2%, and 3%).

2.2. Sample Preparation

Low-heat skimmed milk powder (DairyAmerica®, Fresno, CA, USA), milk protein concentrate (DairyAmerica®, Fresno, CA, USA), and whey powder (Colun®, La Unión, Chile) were used to achieve the target protein concentrations (4.2%, 4.5%, and 4.8%). Required amounts were calculated via mass balance using the Solver tool in Microsoft Excel 2021. For each treatment, 3 kg of reconstituted milk containing 12% total solids (w/w) was prepared by dissolving the powders in distilled water at 40 °C under magnetically stirring for 15 min at 150 rpm (Agimatic-E, JP. Selecta, Barcelona, Spain), followed by a 30-minute rest to allow for proper hydration of the milk components [28].

2.3. Inoculum Preparation

The mother culture was prepared using a freeze-dried starter culture (SACCO LYOFAST Y456B; Danisco, Italy), formulated to ferment 100 kg of milk per pouch. One pouch was activated in 1 kg of previously pasteurised and cooled (4 °C) reconstituted milk. Finally, it was divided into 30 g portions in sterile containers and stored at −15 °C until use. On the day of fermentation, the required portions were thawed at 25 °C for 25 min and used as inoculum.

2.4. Yogurt Fermentation Process

Reconstituted milk with target protein concentrations (4.2%, 4.5%, and 4.8%) was pasteurized at 80 °C for 25 min, then cooled to the designated fermentation temperatures (36, 40, and 44 °C), and transferred to a pre-sanitized jacketed kettle equipped with a temperature control system to maintain the desired fermentation conditions. Following a 5 min temperature stabilization period, the milk was inoculated (1%, 2%, or 3%) with the thawed starter culture (previously equilibrated at 25 °C for 15 min) and stirred manually with a spatula for 1 min. Data acquisition of the physicochemical parameters began immediately upon inoculum addition and continued until the pH reached 4.6.

2.5. Physicochemical Analysis of Yogurt During Fermentation

Physicochemical parameters, including pH, titratable acidity, and colour, were monitored at 10-minute intervals throughout the fermentation process.

2.5.1. pH Measurement

Before each test, the electrode connected to the digital potentiometer (model PH818) was calibrated separately using standard buffer solutions of pH = 7.00 and pH = 4.01 at the corresponding test temperatures. Once calibration was completed, the pH electrodes were stored in the storage solutions recommended by the manufacturers.

For each measurement, 10 mL of sample was collected and placed in a 50 mL beaker. The sample was stirred, and the pH was measured using the aforementioned equipment. After the analysis, all samples were discarded in a designated waste container.

2.5.2. Lactic Acid Concentration Measurement

The acidity resulting from the metabolic activity of lactic acid bacteria was quantified using acid–base titration. For each measurement, 10 g of the sample were collected and cooled to 25 °C to minimize microbial activity. Three drops of 1% phenolphthalein solution were then added as an indicator, and the titration was performed using 0.1 N sodium hydroxide (NaOH) until a persistent pale pink colour appeared [29]. Titratable acidity was calculated as lactic acid, the primary organic acid in yogurt samples, using the following equation:

$$\% \text{ Lactic acid} = \frac{(\text{mlNaOH}) \times (\text{N}) \times (\text{mEq})}{\text{sample weight}} \times 100 \quad (1)$$

where

- ml NaOH: Volume of NaOH used;
- N: Normality of NaOH (0.1);
- mEq: Milliequivalent of lactic acid (mEq = 0.09);
- Sample weight (g).

2.5.3. Colour Measurement in the CIELAB System

Colour was evaluated using the method described by McDermott et al. [30], with appropriate modifications, employing a portable colourimeter (model WR-10QC, CTI, Shenzhen, China). This device features an automatic calibration function upon start-up using an internal white reference plate. For each measurement, 10 mL samples were placed in a transparent quartz cuvette to allow light transmission. Readings were taken for lightness (L*, 0 = black to 100 = white), a* (green to red hue), and b* (blue to yellow hue). Due to the variation in fermentation time among treatments, the total number of colour measurements per trial varied accordingly, with data collected at 10-minute intervals throughout each fermentation process.

2.6. Model Design, Training, and Implementation

In the present study, artificial neural network (ANN) models were developed with the objective of predicting key physicochemical parameters, specifically pH and titratable acidity, in fermented milk samples. The ANN architecture was structured into three main components. The input layer consisted of seven independent variables: fermentation temperature; inoculum concentration; milk protein concentration; sampling time; and the CIELAB colour values L*, a*, and b*. For the hidden layers, 40 architectural configurations were systematically evaluated, varying the number of hidden layers (1, 2, 4, 6, and 8) and the number of neurons per layer (4, 8, 12, 16, 20, 24, 28, and 32). Each configuration was treated as an independent model. The output layer consisted of a single neuron, responsible for estimating the target variable (either pH or titratable acidity). Prior to training, the experimental data were normalized to the [0, 1] range using a min–max transformation and subsequently split into training (90%) and validation (10%) sets.

Model development and simulation were carried out in the Python environment (version 3.13), using the implementation of the multilayer perceptron (MLP). The training process was conducted using the backpropagation algorithm, optimized with the Adam (adaptive moment estimation) algorithm, with a fixed learning rate of 0.1. Each model was trained for 500 full epochs. The performance of the neural networks was evaluated using widely adopted statistical metrics in the field of machine learning: mean absolute percentage error (MAPE), root mean squared error (RMSE), and the coefficient of determination (R^2).

According to the criteria established by Batista et al. [24], the optimal models were selected based on the highest R^2 value and the lowest RMSE. As a result, two final models with high accuracy were identified: one specialized in predicting pH and the other in estimating titratable acidity. The predictive validity of the models was confirmed using a linear regression analysis between the predicted and experimental values, yielding high coefficients of determination (R^2), which support the robustness and reliability of the developed models.

3. Results and Discussion

3.1. Monitoring of pH During Yogurt Fermentation

The pH profiles of yogurts prepared under varying fermentation temperatures, protein concentrations, and inoculum percentages are shown in Figure 1. Two distinct phases can be identified in the pH decline curves: the first corresponds to the lag phase, characterised by a slow decrease in pH (values above 5.8), while the second corresponds to the logarithmic phase, during which the pH rapidly decreases to a value near 4.6. In the yogurt industry, a pH of approximately 4.6 is considered the typical endpoint of fermentation, as it coincides with the isoelectric point of casein, where the protein loses its net charge, becomes destabilised, and precipitates, leading to gel or curd formation [31]. Both fermentation phases were clearly observed in this study. However, other authors have reported an additional third stage, known as the deceleration phase of acidification, which occurs below the isoelectric point of casein [32]. This final phase could not be observed, probably because the culture had not produced enough acid or depleted the lactose, meaning it had not yet entered self-inhibition or slowdown; therefore, the late plateau falls outside the monitoring window

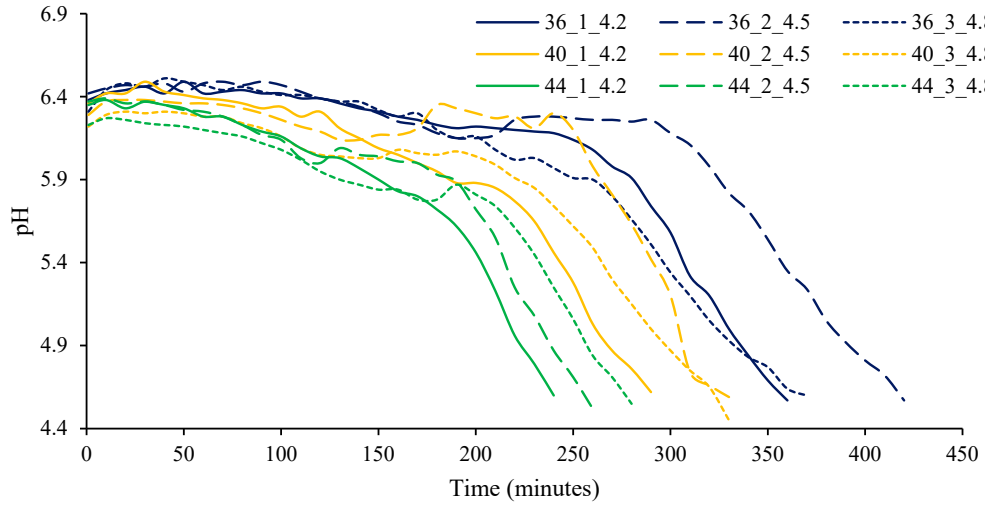

Figure 1. pH variation profile under different fermentation conditions. Note: "36_2_4.2" refers to a fermentation at 36 °C, 2% starter concentration, and 4.8% protein content.

Furthermore, the fermentation temperature had a significant influence ($p < 0.05$) on the duration of the process. At 36 °C, fermentation proceeded more slowly, with an approximate duration of 7 h, whereas at 44 °C, the process was significantly faster, reaching completion in approximately 4.5 h. These findings are consistent with previous studies [31,32]. The duration of the fermentation process is closely linked to the metabolic activity of lactic acid bacteria, which increases at higher temperatures. Under such conditions, the bacteria produce lactic acid at an accelerated rate, resulting in a rapid decline in pH [33].

A trend was also observed whereby an increase in protein concentration led to a prolonged total fermentation time. This behaviour may be associated with the fact that the protein adjustment was primarily achieved through the addition of whey proteins, resulting in an imbalance in the natural casein-to-whey protein ratio. Such a disproportion may have influenced the acidification kinetics, as denatured whey proteins are known to interact with casein micelles, thereby altering the gelation conditions. Moreover, it has been reported that these proteins lower the functional gelation pH (approximately pH 5.2) and exhibit significant buffering capacity, mitigating pH changes by neutralizing the protons generated during acidification [34].

On the other hand, both a higher inoculum percentage and elevated fermentation temperatures exhibited a significant effect in accelerating the pH decline and reducing the time required to reach gelation. Similar findings have been previously reported by other authors [35]. This effect may be explained by the increased concentration of viable lactic acid bacteria, which enhances lactose metabolism and, consequently, lactic acid production. Moreover, it has been suggested that temperatures above 40 °C promote the rapid growth of lactic acid bacteria, thereby increasing the acidification rate [12]. However, this phenomenon may compromise the quality of the final product by promoting the formation of structurally weak gels, increasing syneresis, and resulting in a more liquid consistency of the yogurt [36].

However, in the present study, a higher inoculum percentage was found to slow down the pH decline and prolong the time required to reach the gelation point. Although several studies report that a high inoculum accelerates fermentation and reduces the time needed to reach the gelation pH (~4.6) [37], the opposite behaviour was observed in our study. This phenomenon could be explained, firstly, by the increased buffering capacity of the system, associated with the addition of whey proteins used to adjust the milk's protein concentration. This enhanced buffering effect delays the decrease in pH, thereby extending the fermentation time. It may also be related to a metabolic self-inhibition effect caused by the high bacterial density. In this case, the rapid production of lactic acid at the beginning of fermentation can lead to the formation of inhibitory compounds such as hydrogen peroxide (H_2O_2) or acetic acid, which in turn inhibit bacterial activity during the logarithmic phase, slowing down the process [38].

3.2. Monitoring of Acidity During Yogurt Fermentation

Throughout the fermentation process, all treatments exhibited a characteristic pattern in the evolution of titratable acidity, which can be described in two distinct phases. The first corresponds to the lag phase, characterised by a low rate of lactic acid production, attributed to the adaptation period of lactic acid bacteria to environmental conditions (nutrient composition, temperature, pH, among others) [39]. This is followed by the exponential growth phase, during which a marked increase in lactic acid production is observed, driven by the rapid proliferation of bacteria and accelerated lactose metabolism [40]. This biphasic pattern is in agreement with that described by Sodini et al. [41], who highlighted the importance of the lag phase in enabling the metabolic adaptation of lactic acid bacteria. Moreover, it has been reported that this initial phase tends to be longer in yogurts produced using skimmed milk [32], followed by an exponential phase during which lactic acid accumulation is rapidly intensified.

Changes in titratable acidity during the fermentation of milk into yogurt are presented in Figure 2. When considered individually, fermentation temperature and inoculum concentration did not exhibit a statistically significant effect ($p > 0.05$) on lactic acid formation. However, the interaction among temperature, inoculum concentration, and protein concentration had a significant impact ($p < 0.05$). For instance, in most treatments, higher

protein concentrations and inoculum combined with lower fermentation temperatures were associated with slower lactic acid production. These findings are consistent with those reported by Kristo et al. [42], who indicated that at temperatures below 40 °C, acidification proceeds more slowly, reducing the rate of lactose conversion into lactic acid. Another possible inhibition of lactic acid production observed at higher protein concentrations may be attributed to microorganisms redirecting part of their metabolic activity towards proteolysis. Furthermore, the lactic acid bacteria used in this study, *Lactobacillus delbrueckii subsp. bulgaricus* and *Streptococcus thermophilus*, may not have reached their optimal temperature for growth and metabolic activity under certain experimental conditions.

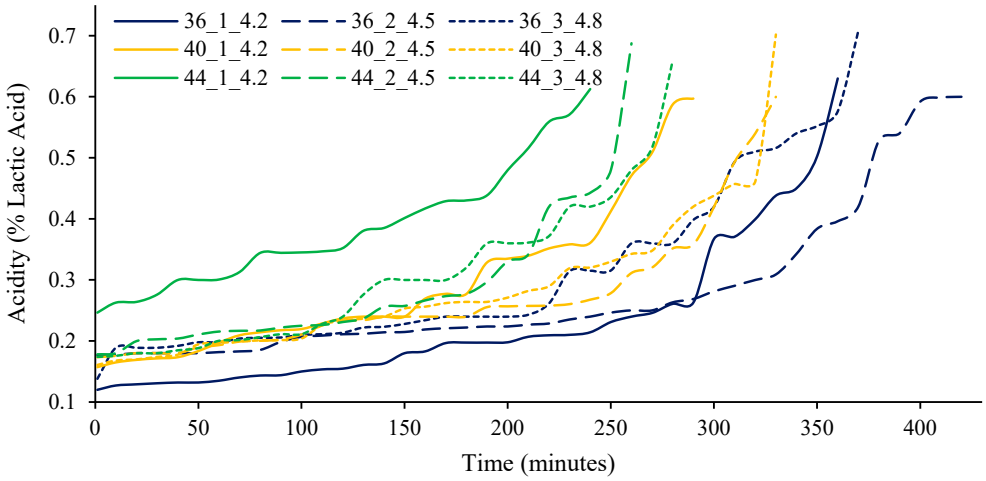

Figure 2. Lactic acid formation as a function of fermentation conditions. Note: "36_2_4.2" refers to a fermentation at 36 °C, 2% starter concentration, and 4.8% protein content.

In all treatments, as shown in the previous figure, the titratable acidity of the yogurts exceeded 0.6%. These values comply with the standards established by dairy industry regulations [43,44], which define this threshold as the minimum requirement for properly fermented yogurt. Furthermore, the values observed are consistent with those reported by Manela et al. [29], supporting the reliability of the fermentation process employed in this study.

3.3. Colour Behaviour During Fermentation

Fermentation temperature and protein concentration significantly influenced the behaviour of the yogurt colour parameters L*, a*, and b*. As shown in Figure 3, a progressive increase in the values of L*, a*, and b* was recorded across all treatments during the fermentation process. At the onset of fermentation, it was evident that higher protein concentrations significantly reduced ($p < 0.05$) lightness (L*), decreasing from 83.62 ± 0.03 to 82.08 ± 0.01 (Figure 3A). This effect may be attributed to the higher proportion of whey proteins added to adjust the overall protein concentration, which alter the colloidal structure of the system. Their presence may be associated with a reduced light-scattering capacity, resulting in decreased perceived brightness in the milk. Simultaneously, a significant increase ($p < 0.05$) was observed in a* values (from −3.60 ± 0.02 to −3.22 ± 0.02) and b* values (from 1.78 ± 0.07 to 2.30 ± 0.03) (Figure 3B,C). This increase in chromatic parameters may be attributed to the formation of melanoidins resulting from Maillard reactions during heat treatment, especially in systems with high protein and lactose concentrations. These reactions produce compounds with yellowish hues. Additionally, the presence of riboflavin—which exhibits a yellow-greenish tone—in both the protein concentrate and whey powder may contribute to the increase in a* and b* values [45]. The L*, a*, and b* values observed in this study are consistent with those reported by Milovanovic et al. [46]

and Cheng et al. [47], although slight variations in chromaticity values were noted, possibly due to the reconstitution of powdered milk with a high protein concentration, as indicated by McDermott et al. [30].

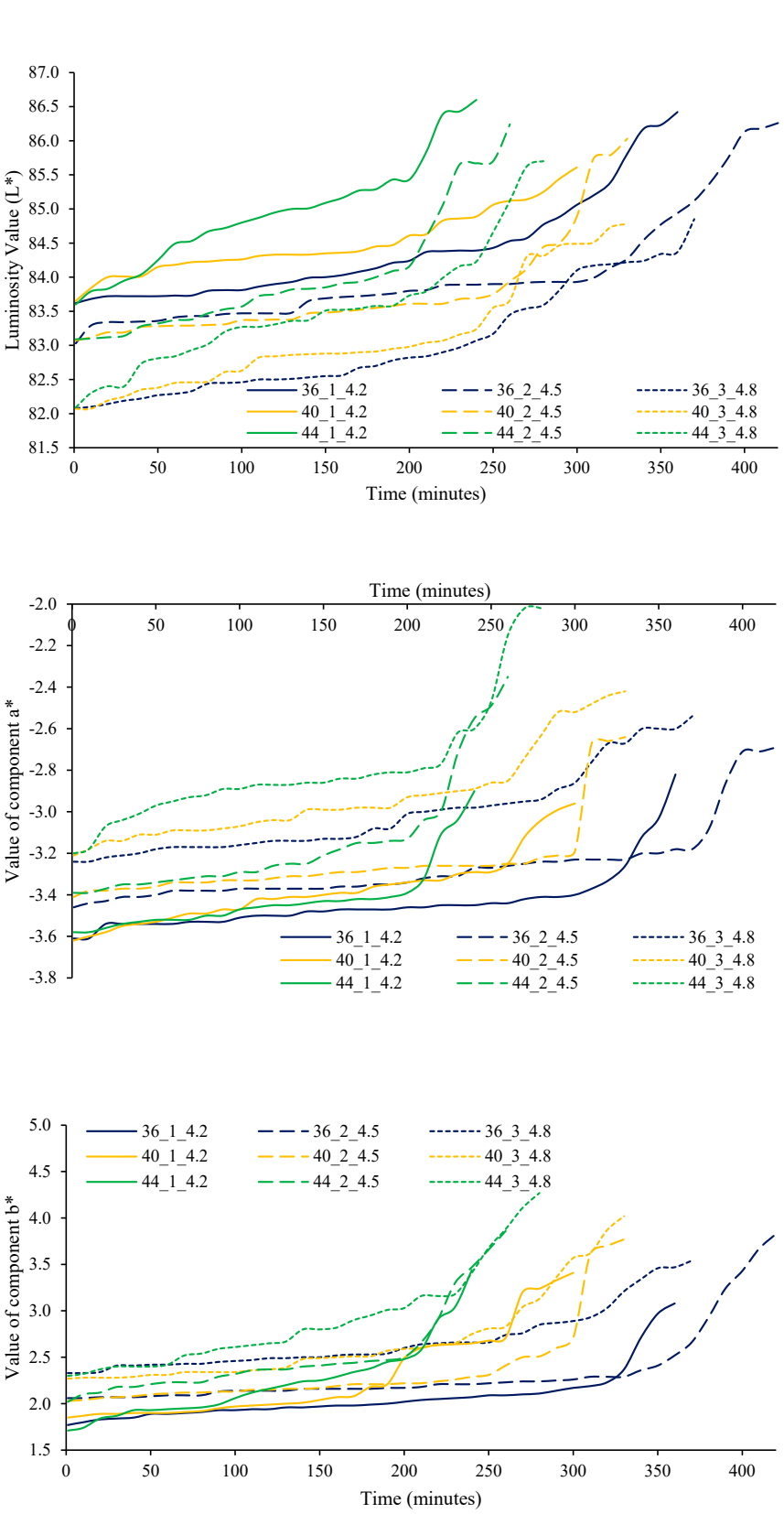

Figure 3. Variation in CIELAB colour parameters during yogurt fermentation: (**A**) L* component, (**B**) a* component, and (**C**) b* component. Note: "36_2_4.2" refers to a fermentation at 36 °C, 2% starter concentration, and 4.8% protein content.

During fermentation, a gradual increase in CIELAB values was observed as milk was transformed into yogurt (Figure 3). At the end of the process, samples with lower protein concentrations exhibited significantly higher lightness (L*) (86.21 ± 0.53, $p < 0.05$) compared to those with higher protein content. Regarding the a* and b* values, yogurt made with 4.2% protein exhibited values of 2.89 ± 0.07 and 3.31 ± 0.20, respectively, whereas the sample with 4.8% protein showed significantly different values of 2.33 ± 0.27 and 3.94 ± 0.37, respectively. These findings align with those reported by Rahman et al. [6], who also observed increases in L*, a*, and b* values during fermentation, which were attributed to physicochemical and structural modifications induced by the metabolic and proteolytic activities of lactic acid bacteria [4,48]. However, Du et al. [49] reported lower lightness (L* = 77.44 ± 0.22), a comparable a* value (−2.99 ± 0.06), and a substantially higher b* value (6.22 ± 0.04) relative to those found in the present study. These discrepancies may be explained by variations in chemical composition, heat treatment applied, and the type of milk used.

The observed increase in L*, a*, and b* values during fermentation is likely attributed to the formation of various compounds such as peptides, amino acids, acetaldehyde, and diacetyl, along with the accumulation of organic acids including lactic, formic, citric, acetic, and butyric acids [11]. These compounds can alter light absorption and scattering, thereby modifying the product's colour parameters. Additionally, protein aggregation induced during fermentation promotes gelation, leading to changes in the yogurt's colloidal structure and its light-scattering capacity, which directly affects lightness (L*). Altogether, the complex biochemical and structural changes occurring during fermentation influence the interaction of light with the final product [50].

3.4. Development of ANN Models for the Prediction of pH and Acidity

Colour data (L*, a*, b*), along with the pH and titratable acidity values recorded during milk fermentation, were used to train a total of 80 artificial neural network (ANN) models: 40 models for pH prediction and 40 for titratable acidity prediction. Each model was trained over 500 epochs. The performance metrics obtained are summarized in Tables 1 and 2, respectively.

Table 1. Performance of the ANN models developed for pH prediction.

Maximum Number of Neurons per Hidden Layer	Performance Metrics	Number of Hidden Layers				
		1	2	4	6	8
4	MAPE	0.129	0.080	0.072	0.331	0.082
	RMSE	0.027	0.011	0.008	0.238	0.012
	R^2	0.885	0.955	0.964	−0.002	0.951
8	MAPE	0.082	0.077	0.075	0.088	0.091
	RMSE	0.011	0.010	0.009	0.012	0.012
	R^2	0.954	0.956	0.961	0.951	0.950
12	MAPE	0.076	0.072	0.070	0.322	0.119
	RMSE	0.010	0.009	0.008	0.240	0.021
	R^2	0.959	0.963	0.967	−0.010	0.910
16	MAPE	0.082	0.070	0.074	0.068	0.320
	RMSE	0.009	0.009	0.009	0.008	0.237
	R^2	0.960	0.964	0.961	0.968	0.000
20	MAPE	0.086	0.078	0.072	0.091	0.319
	RMSE	0.010	0.010	0.008	0.014	0.242
	R^2	0.957	0.957	0.965	0.942	−0.019

Table 1. *Cont.*

Maximum Number of Neurons per Hidden Layer	Performance Metrics	Number of Hidden Layers				
		1	**2**	**4**	**6**	**8**
24	MAPE	0.895	0.914	0.876	0.895	−0.053
	RMSE	0.078	0.077	0.080	0.323	0.324
	R^2	0.959	0.961	0.952	−0.011	−0.016
28	MAPE	0.074	0.102	0.319	0.319	0.322
	RMSE	0.008	0.007	0.238	0.244	0.237
	R^2	0.965	0.969	−0.001	−0.030	0.000
32	MAPE	0.076	0.072	0.321	0.320	0.319
	RMSE	0.009	0.009	0.244	0.245	0.239
	R^2	0.961	0.963	−0.029	−0.031	−0.008

Table 2. Performance of the ANN models developed for titratable acidity prediction.

Maximum Number of Neurons per Hidden Layer	Performance Metrics	Number of Hidden Layers				
		1	**2**	**4**	**6**	**8**
4	MAPE	0.036	0.036	0.105	0.105	0.107
	RMSE	0.002	0.002	0.018	0.019	0.017
	R^2	0.862	0.862	0.064	0.149	0.020
8	MAPE	0.035	0.041	0.037	0.106	0.105
	RMSE	0.002	0.003	0.002	0.018	0.019
	R^2	0.864	0.822	0.855	0.071	0.105
12	MAPE	0.036	0.036	0.105	0.105	0.106
	RMSE	0.002	0.002	0.020	0.017	0.017
	R^2	0.852	0.858	0.183	0.031	0.002
16	MAPE	0.037	0.036	0.037	0.105	0.106
	RMSE	0.003	0.002	0.002	0.018	0.018
	R^2	0.852	0.853	0.855	0.053	0.061
20	MAPE	0.036	0.105	0.039	0.106	0.105
	RMSE	0.002	0.018	0.003	0.018	0.019
	R^2	0.866	0.058	0.829	0.039	0.107
24	MAPE	0.040	0.042	0.113	0.105	0.105
	RMSE	0.003	0.003	0.026	0.019	0.018
	R^2	0.829	0.808	0.539	0.118	0.085
28	MAPE	0.105	0.105	0.108	0.053	0.105
	RMSE	0.018	0.017	0.017	0.005	0.017
	R^2	0.060	0.023	0.009	0.734	0.026
32	MAPE	0.105	0.105	0.035	0.105	0.105
	RMSE	0.017	0.019	0.002	0.019	0.019
	R^2	0.004	0.139	0.868	0.102	0.141

Table 1 presents a model comprising two hidden layers, each containing 28 neurons (highlighted in grey), which achieved a coefficient of determination (R^2) of 0.969 and a mean squared error (RMSE) of 0.007 pH units. These metrics reflect a high level of accuracy and strong predictive performance for estimating pH during yogurt fermentation, as illustrated in Figure 4A. Conversely, Table 2 outlines an optimised model for predicting titratable

acidity, consisting of four hidden layers with 32 neurons in each (highlighted in grey). This model attained an R^2 of 0.868 and an RMSE of 0.002 (lactic acid %), demonstrating its effectiveness in tracking the progression of acidity throughout the fermentation process, as shown in Figure 4B.

(A)

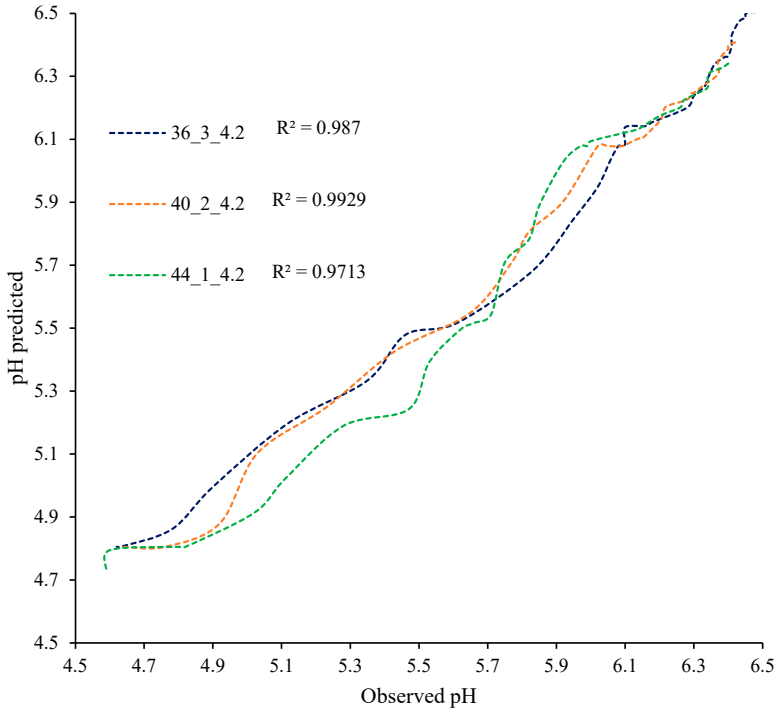

(B)

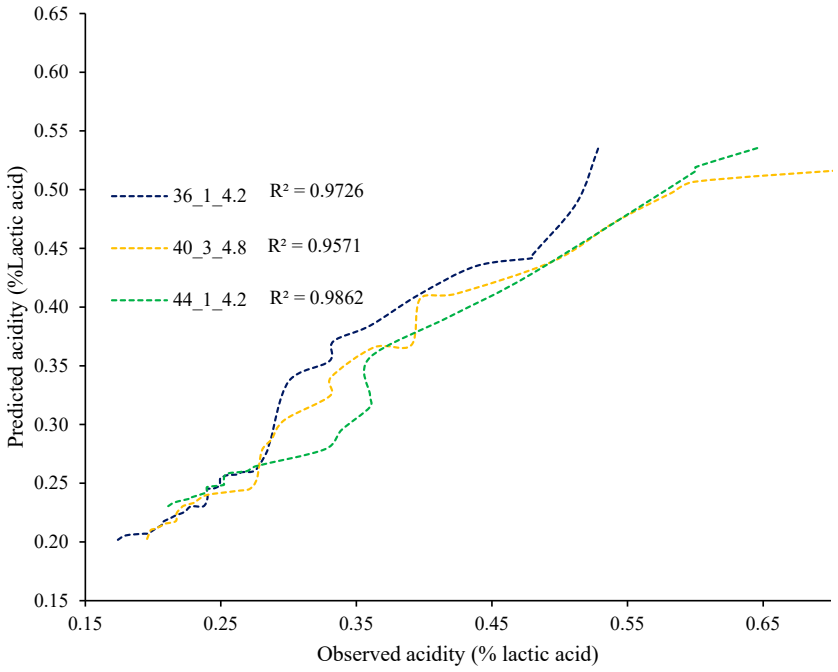

Figure 4. Relationship between experimental and predicted values versus estimated values (ANN model): (**A**) pH and (**B**) titratable acidity. Note: "36_1_4.2" refers to a fermentation at 36 °C, 1% starter concentration, and 4.8% protein content.

The high degree of correlation obtained during model training suggests that variations in the CIELAB colour parameters are closely associated with the accumulation of lactic acid and, consequently, the reduction in pH. This underscores the potential of colour monitoring as a non-invasive indicator of fermentation progress. This trend is consistent with the findings of Ramezani et al. [51], who also reported a strong correlation between optical parameters and physicochemical changes during the fermentation process.

To date, most research has concentrated on developing predictive models using chemometric techniques. For instance, Aliakbarian et al. [52] developed a model based on partial least squares (PLS) regression combined with genetic algorithms (GA) to estimate yogurt age from UV–VIS spectra. Similarly, Arango et al. [53] employed near-infrared (NIR) light backscattering in conjunction with regression techniques, achieving a strong correlation between the signal (R) and pH, with an R^2 exceeding 0.993. This predictive model was validated with high accuracy (R^2 up to 0.998), establishing it as a reliable and non-invasive tool for real-time pH monitoring during fermentation [16]. In another study, the combination of NIR spectroscopy and aquaphotomics analysis with principal component analysis (PCA) yielded exceptionally high R^2 values, typically above 0.95, for predicting both pH and titratable acidity [31]. Although these models demonstrated greater accuracy than those developed in the present study, the use of NIR spectra likely offers a more detailed characterisation of physicochemical changes compared to analyses based solely on the visible spectrum. Nevertheless, the models proposed in this research, based on CIELAB colour parameters and artificial neural networks (ANNs), also exhibited strong predictive performance for both pH and titratable acidity.

This is illustrated in Figure 4A,B, which display the model fits developed using 90% of the data, applied to a randomly selected trial. Both models achieved R^2 values exceeding 0.97 for the evaluated parameters (pH and titratable acidity), demonstrating an excellent fit to the experimental data. Although these results reflect a high predictive capacity, the potential risk of overfitting should be considered. Nevertheless, the integration of these technologies supports their feasibility as an innovative, accurate, and non-destructive strategy for the continuous monitoring of the fermentation process.

In this context, the integration of CIELAB colour parameters with artificial neural network (ANN) algorithms offers a viable, precise, and adaptable approach for estimating pH and titratable acidity during yogurt fermentation. This combination enables the inclusion of multiple variables, dynamic adjustment to changing process conditions, and enhanced operational efficiency. Unlike traditional analytical methods, which require frequent sampling, specialised personnel, and ongoing calibration, these intelligent tools provide greater consistency in process control, improve final product quality, and significantly reduce operational costs. Moreover, the models were developed taking into account varying levels of protein, temperature, and inoculum, thereby extending their applicability to real industrial environments, where production conditions may differ considerably between facilities.

4. Conclusions

The results of this study demonstrate that models based on artificial neural networks (ANNs) are highly effective tools for predicting pH and titratable acidity during yogurt fermentation, using colour parameters in the CIELAB space as input variables. The optimal models, configured with two hidden layers and 28 neurons per layer for pH prediction and four hidden layers with 32 neurons per layer for acidity prediction, achieved excellent levels of accuracy. These findings confirm the strong correlation between colour variations (L*, a*, b*) and the physicochemical changes associated with lactic acid accumulation and pH reduction throughout the fermentation process. Moreover, the predictive capability of these models under varying operating conditions including differences in protein con-

centration, inoculum level, and fermentation temperature, supporting their potential for application in industrial settings, where process standardisation and quality control are essential to ensure consistency and production efficiency.

The implementation of such models allows for real-time, continuous, and non-destructive monitoring, addressing the limitations of traditional measurement techniques (periodic sampling) that require frequent calibration and carry a risk of contamination. As a result, the integration of artificial neural networks with optical methods based on the CIELAB system emerges as a highly promising strategy for automated process control. This approach not only enhances resource efficiency but also contributes to reducing production costs.

Author Contributions: Conceptualization, U.A. and M.C.; methodology, U.A. and M.C.; software, J.T. and E.G.R.; validation, J.T., E.G.R. and H.C.; formal analysis, U.A., J.T. and N.C.R.; investigation, U.A., J.T. and H.C.; resources, U.A., M.C. and A.C.; data curation, J.T., H.C. and N.C.R.; writing—original draft preparation, U.A. and J.T.; writing—review and editing, M.C., C.V.-S. and E.G.R.; visualization, C.V.-S. and A.C.; supervision, U.A. and M.C.; project administration, A.C.; funding acquisition, U.A. and M.C. All authors have read and agreed to the published version of the manuscript.

Funding: This research was supported by the Consejo Nacional de Ciencia, Tecnología e Innovación Tecnológica (CONCYTEC) and the Programa Nacional de Investigación Científica y Estudios Avanzados (PROCIENCIA), under Contrato N° PE501082973-2023.

Institutional Review Board Statement: Not applicable.

Informed Consent Statement: Not applicable.

Data Availability Statement: The original contributions presented in this study are included in the article; further inquiries can be directed to the corresponding author.

Acknowledgments: The authors would like to the Universidad Nacional del Altiplano and the Instituto de Investigacion e Innovación en Producción, Seguridad Alimentaria y Agroindustria—IPSAA, Puno, Perú, for allowing us to use their laboratory and equipment during the execution of the project.

Conflicts of Interest: The authors declare no conflicts of interest.

References

1. Marete, P.K.; Mariga, A.M.; Huka, G.; Musalia, L.; Marete, E.; Mathara, J.M.; Arimi, J.M. Effects of Optimizing Fermentation Time and Stabilizers Using Response Surface Methodology on Physicochemical Properties of Camel Milk Yoghurt. *Appl. Food Res.* **2024**, *4*, 100469. [CrossRef]
2. Lim, T.W.; Lim, R.L.H.; Pui, L.P.; Tan, C.P.; Ho, C.W. Evaluating the Potential of Stabilised Betacyanins from Fermented Red Dragon Fruit (*Hylocereus polyrhizus*) Drink: Sustainable Colouration and Antioxidant Enhancement of Stirred Yoghurt. *Future Foods* **2024**, *10*, 100452. [CrossRef]
3. Zhang, X.; Zheng, Y.; Zhou, C.; Cao, J.; Zhang, Y.; Wu, Z.; Pan, D.; Cai, Z.; Xia, Q. Combining Thermosonication Microstress and Pineapple Peel Extract Addition to Achieve Quality and Post-Acidification Control in Yogurt Fermentation. *Ultrason. Sonochem.* **2024**, *105*, 106857. [CrossRef]
4. Akarca, G.; Denizkara, A.J. Changes of Quality in Yoghurt Produced under Magnetic Field Effect during Fermentation and Storage Processes. *Int. Dairy J.* **2024**, *150*, 105841. [CrossRef]
5. Ouyang, K.; Xie, H.; Wu, K.; Xiong, H.; Zhao, Q. Improving Fermented Milk Products Using PH-Responsive Whey Protein Fibrils: A Case Study on Stirred Yogurt. *Food Biosci.* **2024**, *60*, 104507. [CrossRef]
6. Rahman, M.S.; Emon, D.D.; Nupur, A.H.; Mazumder, M.A.R.; Iqbal, A.; Alim, M.A. Isolation and Characterization of Probiotic Lactic Acid Bacteria from Local Yogurt and Development of Inulin-Based Synbiotic Yogurt with the Isolated Bacteria. *Appl. Food Res.* **2024**, *4*, 100457. [CrossRef]
7. Du, H.; Wang, X.; Yang, H.; Zhu, F.; Cheng, J.; Peng, X.; Lin, Y.; Liu, X. Effects of Mulberry Pomace Polysaccharide Addition before Fermentation on Quality Characteristics of Yogurt. *Food Control* **2023**, *153*, 109900. [CrossRef]
8. Wang, R.; Ma, C.; Wang, K. Comparison of the Physicochemical Property and Volatile Flavour Compounds of Yoghurt Made from Ultra-Pasteurised and Membrane-Filtered Milk. *LWT* **2024**, *203*, 116338. [CrossRef]

9. Li, D.; Cui, Y.; Wu, X.; Li, J.; Min, F.; Zhao, T.; Zhang, J.; Zhang, J. Graduate Student Literature Review: Network of Flavor Compounds Formation and Influence Factors in Yogurt. *J. Dairy Sci.* **2024**, *107*, 8874–8886. [CrossRef] [PubMed]
10. Miranda-Mejía, G.A.; Martín del Campo-Barba, S.T.; Arredondo-Ochoa, T.; Tejada-Ortigoza, V.; Morales-de la Peña, M. Low-Intensity Pulsed Electric Fields Pre-Treatment on Yogurt Starter Culture: Effects on Fermentation Time and Quality Attributes. *Innov. Food Sci. Emerg. Technol.* **2024**, *95*, 103708. [CrossRef]
11. Yankey, S.; Mensah, E.O.; Ankar-Brewoo, G.M.; Ellis, W.O. Optimized Fermentation Conditions for Dragon Fruit Yogurt. *Food Humanit.* **2023**, *1*, 343–348. [CrossRef]
12. Pacco, H.C. Simulation in the Temperature Parameters Control in the Yogurt Manufacturing Process. *Procedia Comput. Sci.* **2023**, *217*, 286–295. [CrossRef]
13. Zhang, L.; Zhou, S.; Zhang, A.; Zhang, H.; Wang, R.; Wang, X.; Hu, Y.; Ma, H.; Zhou, C. Green Efficient Preparation and On-Line Monitoring: Hybrid Effect of Okra Pectin and Controlled-Temperature Ultrasound on Physicochemical Properties of Low-Fat Yogurt. *J. Food Eng.* **2024**, *370*, 111963. [CrossRef]
14. Zang, J.; Pan, X.; Zhang, Y.; Tu, Y.; Xu, H.; Tang, D.; Zhang, Q.; Chen, J.; Yin, Z. Mechanistic Insights into Gel Formation of Egg-Based Yoghurt: The Dynamic Changes in Physicochemical Properties, Microstructure, and Intermolecular Interactions during Fermentation. *Food Res. Int.* **2023**, *172*, 113097. [CrossRef] [PubMed]
15. Gorla, G.; Ferrer, A.; Giussani, B. Process Understanding and Monitoring: A Glimpse into Data Strategies for Miniaturized NIR Spectrometers. *Anal. Chim. Acta* **2023**, *1281*, 341902. [CrossRef]
16. Liu, S.; Contreras, F.; Alemán, R.S.; Fuentes, J.M.; Arango, O.; Castillo, M. Validation of an Optical Technology for the Determination of PH in Milk during Yogurt Manufacture. *Foods* **2024**, *13*, 2766. [CrossRef]
17. García-Pérez, F.J.; Lario, Y.; Fernández-López, J.; Sayas, E.; Pérez-Alvarez, J.A.; Sendra, E. Effect of Orange Fiber Addition on Yogurt Color during Fermentation and Cold Storage. *Color Res. Appl.* **2005**, *30*, 457–463. [CrossRef]
18. Nayak, J.; Vakula, K.; Dinesh, P.; Naik, B.; Pelusi, D. Intelligent Food Processing: Journey from Artificial Neural Network to Deep Learning. *Comput. Sci. Rev.* **2020**, *38*, 100297. [CrossRef]
19. Denholm, S.J.; Brand, W.; Mitchell, A.P.; Wells, A.T.; Krzyzelewski, T.; Smith, S.L.; Wall, E.; Coffey, M.P. Predicting Bovine Tuberculosis Status of Dairy Cows from Mid-Infrared Spectral Data of Milk Using Deep Learning. *J. Dairy Sci.* **2020**, *103*, 9355–9367. [CrossRef] [PubMed]
20. Safari, R.; Sheikhlou, M.; Esmaeilpour, M.; Jafarzadeh, H.; Pour, A.S. Application of Artificial Neural Networks to Predict Milk Production in Holstein Cows. *J. Rumin. Res.* **2024**, *12*, 111–128.
21. Bisutti, V.; Mota, L.F.M.; Giannuzzi, D.; Toscano, A.; Amalfitano, N.; Schiavon, S.; Pegolo, S.; Cecchinato, A. Infrared Spectroscopy Coupled with Machine Learning Algorithms for Predicting the Detailed Milk Mineral Profile in Dairy Cattle. *Food Chem.* **2024**, *461*, 140800.
22. Zedda, L.; Perniciano, A.; Loddo, A.; Di Ruberto, C. Understanding Cheese Ripeness: An Artificial Intelligence-Based Approach for Hierarchical Classification. *Knowl. Based Syst.* **2024**, *295*, 111833. [CrossRef]
23. Bi, K.; Qiu, T.; Huang, Y. A Deep Learning Method for Yogurt Preferences Prediction Using Sensory Attributes. *Processes* **2020**, *8*, 518. [CrossRef]
24. Batista, L.F.; Marques, C.S.; Pires, A.C.d.S.; Minim, L.A.; Soares, N.d.F.F.; Vidigal, M.C.T.R. Artificial Neural Networks Modeling of Non-Fat Yogurt Texture Properties: Effect of Process Conditions and Food Composition. *Food Bioprod. Process.* **2021**, *126*, 164–174. [CrossRef]
25. Sofu, A.; Ekinci, F.Y. Estimation of Storage Time of Yogurt with Artificial Neural Network Modeling. *J. Dairy Sci.* **2007**, *90*, 3118–3125. [CrossRef]
26. Aït-Kaddour, A.; Abdelbaky, H.M.; Hamdy, S.M.; Boubellouta, T.; Abou-El-Karam, S.; Abdelmentolb, H.S. Discrimination of Thermally Treated Milk Using Fluorescence Spectroscopy Combined with PCA and Artificial Neural Networks. *J. Food Compos. Anal.* **2025**, 107952. [CrossRef]
27. Tarr, B.; Tőzsér, J.; Szabó, I.; Revoly, A. Estimation of Milk Casein Content Using Machine Learning Models and Feeding Simulations. *Dairy* **2025**, *6*, 35. [CrossRef]
28. Alvarado, U.; Zamora, A.; Arango, O.; Saldo, J.; Castillo, M. Prediction of Riboflavin and Ascorbic Acid Concentrations in Skimmed Heat-Treated Milk Using Front-Face Fluorescence Spectroscopy. *J. Food Eng.* **2022**, *318*, 110869. [CrossRef]
29. Matela, K.S.; Pillai, M.K.; Thamae, T. Evaluation of PH, Titratable Acidity, Syneresis and Sensory Profiles of Some Yoghurt Samples from the Kingdom of Lesotho. *Food Res.* **2019**, *3*, 693–697. [CrossRef] [PubMed]
30. McDermott, A.; Visentin, G.; McParland, S.; Berry, D.P.; Fenelon, M.A.; De Marchi, M. Effectiveness of Mid-Infrared Spectroscopy to Predict the Color of Bovine Milk and the Relationship between Milk Color and Traditional Milk Quality Traits. *J. Dairy Sci.* **2016**, *99*, 3267–3273. [CrossRef] [PubMed]
31. Muncan, J.; Tei, K.; Tsenkova, R. Real-Time Monitoring of Yogurt Fermentation Process by Aquaphotomics near-Infrared Spectroscopy. *Sensors* **2020**, *21*, 177. [CrossRef]

32. Soukoulis, C.; Panagiotidis, P.; Koureli, R.; Tzia, C. Industrial Yogurt Manufacture: Monitoring of Fermentation Process and Improvement of Final Product Quality. *J. Dairy Sci.* **2007**, *90*, 2641–2654. [CrossRef] [PubMed]
33. De Brabandere, A.G.; De Baerdemaeker, J.G. Effects of Process Conditions on the PH Development during Yogurt Fermentation. *J. Food Eng.* **1999**, *41*, 221–227. [CrossRef]
34. Hovjecki, M.; Radovanovic, M.; Miloradovic, Z.; Barukcic Jurina, I.; Mirkovic, M.; Sredovic Ignjatovic, I.; Miocinovic, J. Fortification of Goat Milk Yogurt with Goat Whey Protein Concentrate—Effect on Rheological, Textural, Sensory and Microstructural Properties. *Food Biosci.* **2023**, *56*, 103393. [CrossRef]
35. Lee, W.J.; Lucey, J.A. Structure and Physical Properties of Yogurt Gels: Effect of Inoculation Rate and Incubation Temperature. *J. Dairy Sci.* **2004**, *87*, 3153–3164. [CrossRef]
36. Lee, W.J.; Lucey, J.A. Formation and Physical Properties of Yogurt. *Asian-Australas J. Anim. Sci.* **2010**, *23*, 1127–1136. [CrossRef]
37. Aldaw Ibrahim, I.; Naufalin, R.; Erminawati; Dwiyanti, H. Effect of Fermentation Temperature and Culture Concentration on Microbial and Physicochemical Properties of Cow and Goat Milk Yogurt. In *Earth and Environmental Science, Proceedings of the 2nd International Conference on Life and Applied Sciences for Sustainable Rural Development, Purwokerto, Indonesia, 20–22 November 2019*; Institute of Physics Publishing: Bristol, UK, 2019; Volume 406.
38. Peng, Y.; Horne, D.S.; Lucey, J.A. Impact of Preacidification of Milk and Fermentation Time on the Properties of Yogurt. *J. Dairy Sci.* **2009**, *92*, 2977–2990. [CrossRef]
39. Aguirre-Ezkauriatza, E.J.; Galarza-González, M.G.; Uribe-Bujanda, A.I.; Ríos-Licea, M.; López-Pacheco, F.; Hernández-Brenes, C.M.; Alvarez, M.M. Effect of Mixing During Fermentation in Yogurt Manufacturing. *J. Dairy Sci.* **2008**, *91*, 4454–4465. [CrossRef] [PubMed]
40. Ge, Y.; Yu, X.; Zhao, X.; Liu, C.; Li, T.; Mu, S.; Zhang, L.; Chen, Z.; Zhang, Z.; Song, Z.; et al. Fermentation Characteristics and Postacidification of Yogurt by Streptococcus Thermophilus CICC 6038 and *Lactobacillus delbrueckii* ssp. Bulgaricus CICC 6047 at Optimal Inoculum Ratio. *J. Dairy Sci.* **2024**, *107*, 123–140. [CrossRef] [PubMed]
41. Sodini, I.; Lucas, A.; Oliveira, M.N.; Remeuf, F.; Corrieu, G. Effect of Milk Base and Starter Culture on Acidification, Texture, and Probiotic Cell Counts in Fermented Milk Processing. *J. Dairy Sci.* **2002**, *85*, 2479–2488. [CrossRef]
42. Kristo, E.; Biliaderis, C.G.; Tzanetakis, N. Modelling of Rheological, Microbiological and Acidification Properties of a Fermented Milk Product Containing a Probiotic Strain of *Lactobacillus paracasei*. *Int. Dairy J.* **2003**, *13*, 517–528. [CrossRef]
43. Gobierno del Perú Decreto Supremo, N.° 007-2017-MINAGRI: Reglamento de La Leche y Productos Lácteos 2017. Available online: https://www.gob.pe/institucion/midagri/normas-legales (accessed on 11 July 2025).
44. Codex Alimentarius Commission. *Codex Standar for Fermented Milks (CXS 243-2003)*; Amended in 2022; FAO/WHO: Rome, Italy, 2022. Available online: https://www.fao.org/fao-who-codexalimentarius (accessed on 11 July 2025).
45. Xiang, J.; Liu, F.; Wang, B.; Chen, L.; Liu, W.; Tan, S. A Literature Review on Maillard Reaction Based on Milk Proteins and Carbohydrates in Food and Pharmaceutical Products: Advantages, Disadvantages, and Avoidance Strategies. *Foods* **2021**, *10*, 1998. [CrossRef]
46. Milovanovic, B.; Tomovic, V.; Djekic, I.; Miocinovic, J.; Solowiej, B.G.; Lorenzo, J.M.; Barba, F.J.; Tomasevic, I. Colour Assessment of Milk and Milk Products Using Computer Vision System and Colorimeter. *Int. Dairy J.* **2021**, *120*, 105084. [CrossRef]
47. Cheng, N.; Barbano, D.M.; Drake, M.A. Effect of Pasteurization and Fat, Protein, Casein to Serum Protein Ratio, and Milk Temperature on Milk Beverage Color and Viscosity. *J. Dairy Sci.* **2019**, *102*, 2022–2043. [CrossRef]
48. Vieira, P.; Pinto, C.A.; Lopes-da-Silva, J.A.; Remize, F.; Barba, F.J.; Marszałek, K.; Delgadillo, I.; Saraiva, J.A. A Microbiological, Physicochemical, and Texture Study during Storage of Yoghurt Produced under Isostatic Pressure. *LWT* **2019**, *110*, 152–157. [CrossRef]
49. Du, H.; Yang, H.; Wang, X.; Zhu, F.; Tang, D.; Cheng, J.; Liu, X. Effects of Mulberry Pomace on Physicochemical and Textural Properties of Stirred-Type Flavored Yogurt. *J. Dairy Sci.* **2021**, *104*, 12403–12414. [CrossRef]
50. Yang, Y.; Zhao, Y.; Xu, M.; Yao, Y.; Wu, N.; Du, H.; Tu, Y. Effects of Strong Alkali Treatment on the Physicochemical Properties, Microstructure, Protein Structures, and Intermolecular Forces in Egg Yolks, Plasma, and Granules. *Food Chem.* **2020**, *311*, 125998. [CrossRef]
51. Ramezani, M.; Ferrentino, G.; Morozova, K.; Scampicchio, M. Multiple Light Scattering Measurements for Online Monitoring of Milk Fermentation. *Foods* **2021**, *10*, 1582. [CrossRef] [PubMed]
52. Aliakbarian, B.; Bagnasco, L.; Perego, P.; Leardi, R.; Casale, M. UV-VIS Spectroscopy for Monitoring Yogurt Stability during Storage Time. *Anal. Methods* **2016**, *8*, 5962–5969. [CrossRef]
53. Arango, O.; Trujillo, A.J.; Castillo, M. Inline Control of Yoghurt Fermentation Process Using a near Infrared Light Backscatter Sensor. *J. Food Eng.* **2020**, *277*, 109885. [CrossRef]